MEASUREMENTS OF MAGNETIC FIELDS IN THE VICINITY OF THE MAGNETOSPHERE AND IN INTERPLANETARY SPACE: PRELIMINARY RESULTS FROM MARINER 4

P. J. Coleman, Jr.
Institute of Geophysics & Planetary Physics
University of California, Los Angeles
Los Angeles 24, California

E. J. Smith
Jet Propulsion Laboratory
Pasadena, California

Leverett Davis, Jr.
California Institute of Technology
Pasadena, California

D. E. Jones
Brigham Young University
Provo, Utah

Work NAS 7-100

Presented

at the

Sixth International Space Science Symposium of COSPAR

Mar del Plata, Argentina

May 17, 1965.

Submitted for publication in Space Research VI

ABSTRACT

Various preliminary results of an analysis of data from the magnetometer on board Mariner 4 are described. The measurements discussed were obtained between 28 November 1964 and April 1965. During the first day of the flight the spacecraft traversed the magnetosphere and the interaction region between the magnetosphere and interplanetary space. Very abrupt changes in the stability of the field were produced at the position of the earth's bow shock. There were at least seven traversals of the shock between 36.6 and 38.6 R_e in a region approximately 105°, on the dawn side, from the earth-sun line. The gross properties of the interplanetary field are summarized by means of distributions, over 27-day periods, of values of the various parameters pertaining to the field. On the average, the field tends to lie along the expected spiral direction, but the distribution of polarities along this direction is found to change. The tendency, observed previously with the Mariner 2 and IMP magnetometers, for the interplanetary field to have a southward (positive θ component) component persists. Very rough estimates of the power spectra of the variations in the field are presented.

INTRODUCTION

The spacecraft, Mariner 4, was launched from Cape Kennedy, Florida at 1922 GMT, November 28, 1964. The trajectory achieved was expected to place the spacecraft within 12,500 km of the position of Mars on July 15, 1965. The instrumentation on board Mariner 4 included a vector, low-field helium magnetometer. In the following, certain of the results obtained from studies of the magnetometer data will be described. The results are preliminary in that only data transmitted by teletype from the tracking stations, so-called 'quick look' data, were employed in the analysis. Also, due to constraints on the length of this report, much of the discussion consists of only summaries of the selected results. More detailed reports are to be published elsewhere.

In the following, the first section is a brief description of the Mariner 4 magnetometer. On the first day of the flight measurements were obtained in the distant magnetosphere, in the tail of the magnetosphere, in the interaction region, and in nearby interplanetary space. These measurements are summarized in the second section. Next, the coordinate system that will be employed in the discussion of the interplaentary measurements is defined and the trajectory of the spacecraft is described. In the next four sections, the measurements of the interplaentary field are discussed in terms of distributions of various parameters.

The observations are compared with those obtained with the Mariner 2 magnetometer.

THE LOW FIELD-VECTOR HELIUM MAGNETOMETER

The Mariner 4 magnetometer is a new instrument of a type that has not been flown on any other spacecraft. It was developed for use on missions that require a wide range of operating temperature, an extended dynamic range (a necessity if a substantial planetary field may be encountered), good absolute accuracy, and high sensitivity (a necessity to study interplanetary magnetic fields during the flight to the planet and to look for small perturbations of the interplanetary field if the planetary field is weak). The Mariner 4 instrument measures fields as large as 625γ ($\pm$360γ referred to any of the three components, 1γ = 10^{-5} gauss) with a limiting noise threshold equivalent to an rms field of 0.1γ. The instrument sensitivity (16.7 mv output for 1.0γ of applied field) is linear to within 0.1% over the full range. This is one aspect of the absolute accuracy which is insured by stability of both the linear characteristic and the null point (the output voltage in the absence of an ambient field) over both an extended temperature range (-25° to $+65^{\circ}$C) and long periods of time. High absolute accuracy is an important requirement for an instrument flown on an attitude-stabilized spacecraft, whereas on a spinning spacecraft, the spin permits an in-flight determination of the zero-field outputs of instruments measuring field components, transverse to the spin axis. When the Mariner program was initiated, the above

specifications equaled or exceeded those of the more conventional fluxgate or second harmonic type of magnetometer (such as was utilized on the Mariner 2 mission) [Smith, Davis, Coleman, Sonett, 1965]. Furthermore, the weight and power requirements of the two kinds of instruments were comparable and there was no reason to suppose that the stringent reliability requirements of the planetary mission could not be satisfied by the newer instrument.

The Mariner 4 instrument is a low-field, vector, helium magnetometer not to be confused with either the rudidium magnetometer [Ruddock, 1961] or the high-field, scalar, helium magnetometer [Keyser, Rice, and Schearer, 1961]. Like the latter two it is a resonance magnetometer in which a specimen gas is examined spectroscopically using optical pumping to detect changes in state caused by the presence of weak magnetic fields. However, the vector helium magnetometer is not an absolute instrument like the others which both produce tones, the frequencies of which are proportional to the field magnitude. Instead, it generates three steady or DC voltages each proportional to a component of the ambient field.

The basic operating principles of the Mariner instrument can be understood with the aid of the simplified schematic shown in Figure 1. The pumping light, 1.08 micron radiation obtained from an electrodeless discharge helium lamp, is circularly polarized and focused on an absorption cell where it is partially

absorbed by metastable helium atoms. Absorption and pumping are observed by an infra-red lead sulfide detector. Since simple Zeeman absorption depends on both the polarization of the resonant radiation and its direction of incidence with regard to the magnetic field, the pumped condition can be destroyed by changing the direction of the magnetic field. When a rotating field is applied to the cell, it causes a periodic variation in the transparency of the gas. A sweep oscillator produces two sinusoidal currents 90° out of phase in two mutually perpendicular sets of Helmholtz coils (represented in the figure by a circle) placed around the absorption cell. This generates a 100γ field rotating at a rate of 50 rps. Empirically it is found that the absorption is proportional to the square of the cosine of the angle between the light beam (optical axis) and the magnetic field. Thus, in the absence of an ambient field, the detector output is a second harmonic of the sweep frequency. If the DC field is present, the detector output contains a component at the sweep frequency whose phase depends on the angle between the optical axis of the sensor and the DC field. The AC amplifier passes a signal containing only the fundamental frequency component which is used to generate, by phase coherent detection, a DC current that is applied to the Helmholtz coils to null the external field. Thus, the magnetometer functions as a closed loop, or feedback system with a resulting improvement in output linearity and stability.

The simplified schematic shows the electronics for a two axis system. The tri-axial Mariner instrument utilizes a time-sharing technique to switch the plane of the sweep vector on alternate rotations from the plane of the diagram to a plane perpendicular to the diagram through the optical axis. This commutation provides essentially simultaneous triaxial measurements when the outputs are sampled at the Mariner 4 data rates.

A photograph of the Mariner 4 magnetometer is shown in Figure 2. The one-pound sensor is on the right. The tri-axial helmholtz coils lie on a 4-inch diameter sphere with the helium lamp and igniter at one end and the detector and a preamplifier at the other. The two modules containing the rest of the electronics weigh 4.5 lb.

THE NEAR-EARTH DATA

Figure 3 contains 10-minute averages of the total field magnitude, $|B|$, and the magnitude of the solar-radial component, $|B_r|$, as a function of universal time or, alternatively, geocentric distance. During this time interval, which began shortly after the magnetometer came on scale and ended just prior to complete altitude stabilization, the Mariner rotated slowly ($\sim$ 2 rev. per hr) about an axis oriented toward the sun. The changing orientation, relative to the ambient field, of the two sensor axes transverse to the sun-oriented axis, allowed the corresponding components of the spacecraft field to be derived. The value of $|B_r|$ was adjusted to agree with the radial component of the unperturbed geomagnetic field near the earth. The three spacecraft field components, which total 28γ at the sensor, were subtracted from the data before $|B|$ was computed.

The data show four distinctly different magnetic regimes separated by transitions designated simply as 1, 2, and 3. The data from nearest the earth to the first transition (at $\sim$ 11 R_e, earth radii) show the same general dependence on geocentric distance as the unperturbed geomagnetic field. The average field from Transition 1 to Transition 2 ($\sim$ 21 R_e) is essentially constant in magnitude with an enhanced radial component that points away from the sun (no directional information is shown in the figure). The smaller (5-10γ) average field in the region between Transitions 2 and 3 is irregular in magnitude and direction. The third transition at $\sim$ 35 R_e is not completely obvious in the

10-minute averages but marks the edge of a zone in which regions of rapidly fluctuating fields alternate with regions of relatively stable fields as will be discussed below.

The locations of the three major transitions along the Mariner trajectory are shown in Figure 4. This figure also contains a sketch showing the asymmetric magnetosphere, consisting of a torus formed by field lines that co-rotate with the earth and an elongated magnetic tail pointing away from the sun [Axford, Petschek, and Siscoe, 1965], and the detached hydromagnetic bow shock [Spreiter and Jones, 1963]. We identify Transition 1 with the boundary between the co-rotating magnetosphere and the tail, Transition 2 with the boundary between the tail and the turbulent magnetosheath, and Transition 3 with the so-called standing shock front.

These boundary locations agree reasonably well with corresponding transitions in the Mariner 4 plasma and energetic particle data as well as with previous field and particle measurements on other spacecraft. The dashed curves in Figure 4 shown the average location of the magnetopause and shock front derived from IMP-1 magnetometer data [Ness, Scearce, and Seek, 1964]. Transition 3 occurs near the extension of the outer contour. Transition 2 lies beyond the inner contour but is generally consistent with the spread in individual boundary penetrations by Explorer 14 [Cahill, 1964], IMP-1 [Ness, Scearce, and Seek, 1964], and Explorer 10 [Heppner, Ness, Skillman, and Scearce, 1963] at approximately the same sun-earth-spacecraft angle.

The innermost transition detected by the Mariner magnetometer appears to be associated with general feature in the distribution of trapped electrons with energies greater than 40 kev. Omni-directional flux contours obtained by Explorer 14 instruments [Frank, Van Allen, and Macagno, 1963] show a bijurcation behind the dawn line at an average geocentric distance of $\sim 9\ R_e$ that is quite likely associated with the change from the magneto-sphere proper to the magnetic tail. Detailed comparisons now in progress suggest that the large scale characteristics of the fields observed by Mariner 4 in the different regions also agree with earlier measurements by Explorers 10, 14, and IMP-1.

The data acquired beyond Transition 3 merit special attention because the important features are associated with the fine structure of the field which is obscured by averaging. Figure 5 is a plot of all the magnetic measurements made during a one hour interval corresponding to the range of geocentric distances between 36 to 38 R_e. No attempt was made to remove the effect of the spacecraft roll which causes sinusoidal variations with periods of $\sim$ 30 minutes in the transverse components, B_X and B_Y. The four tri-axial measurements each 12.6 seconds reveal regions of higher noise levels that alternate with regions of relative quiet. The last such observation comes at 0718 and is not shown.

We identify the abrupt changes from one region (TR, the

transition region) to the other (IP, interplanetary space) with successive passages through the shock front (SF). This interpretation is supported by the Mariner plasma measurements which show penetrations into the free-streaming solar wind coincident with several of the SF transitions in the magnetometer data [Dr. C. W. Snyder, private communication]. The multiple passages through the shock front suggest that it is not stationary, but surges back and forth over distances of several earth radii with typical periods of 5 to 20 minutes, at least for this time and location. These results seem quite reasonable as it has been suggested that hydromagnetic shocks resemble hydraulic phenomena in which irregular and fluctuating fronts with considerable structure and precursors ahead of the main shock are typical. The sharp nature of most of the observed transitions suggests that the shock front makes a large angle with the trajectory and moves considerably, rather than that the trajectory lies nearly tangent to the front. Presumably it is the unknown velocity of motion of the front, not the known velocity of the spacecraft, that determines the apparent duration of the crossing from one region to the other. The average interval between successive observations of the shock is comparable to the time required for the solar wind to slide around the magnetosphere so it is not clear whether the local variations in the position of the front are caused by fine structure in the solar wind or by some form of instability.

The outstanding feature of the magnetic data is the occurrence of irregular fields behind the shock with or without an accompanying change in average field magnitude. The same feature was used to identify the IMP-1 shock front locations [Ness, Scearce, and Seek, 1964] and is also obvious in the OGO-1 search coil magnetometer data [McLeod, Holzer, and Smith, 1965]. The fluctuations are very roughly five times as great as outside. Preliminary inspection of tabulated data indicates that periods of 10 seconds or more are prominent in the fluctuations in the transition region but that periods of 2 to 4 seconds or shorter are much less important. Since the field must be convected with the solar wind velocity, the length scale of the irregularities should be of the order of $10^{3.5}$ km times the period in seconds. There is also a noticeable oscillation (not shown) with a period of 2 or 3 minutes (which corresponds to a length of the order of the radius of curvature of the magnetopause) and an amplitude of several gamma.

PREFACE TO THE DISCUSSION OF THE INTERPLANETARY MAGNETIC FIELD

In the following discussion of the interplanetary field, unless otherwise specified, the coordinate system of reference is a spherical system with coordinates r, θ, and φ. The polar axis of this system lies along the axis of rotation of the sun in the direction of the angular velocity vector or roughly northward. The line of reference for the angle φ is defined by the right ascending node of the intersection of the solar equatorial plane with the ecliptic plane. Parameters of the trajectory of Mariner 4 are plotted in Figures 6 and 7. The magnetic field components at the point (r, θ, φ) are B_r, B_θ, and B_φ, where B_r is the component outward from the sun, B_φ is parallel to the solar equatorial plane and positive in the direction of planetary motion, and B_θ completes the right handed system.

The fields of the spacecraft were measured before the flight. They were also checked during the flight using the following procedure: During the first day of the flight, the spacecraft was allowed to roll about an axis coincident with the sun-spacecraft line. The two components of the spacecraft field transverse to the roll axis were checked using the data taken during this 'roll' period. The third component, held parallel to the sun-spacecraft line during the entire flight, was checked by assuming trial values and obtaining, for each value, a

distribution over a 27-day period for the spiral angle $\alpha_B = \tan^{-1}(-B_\varphi/B_r)$. The value selected was that which provided the distribution most symmetrical about $\alpha_B \approx 50^\circ$ with peaks at $\alpha_B \approx 50^\circ$ and $\alpha_B \approx 50^\circ + 180^\circ$. This requirement fixed the value of the roll-axis component within $\pm(1/3)\gamma$. The selected value of 50° is consistent with the values of the solar wind velocity measured with the Mariner 4 plasma probe.

THE MAGNITUDE OF THE INTERPLANETARY FIELD

Figure 8 contains plots of the distributions of the recorded values of B_r, B_θ, B_φ, and B that were obtained during Solar Rotation Period 1799, 7 January through 2 February 1965. Also shown are distributions of the values of the field strength, B, and of the magnitude of the component transverse to the radial direction, $B_P = (B_\theta^2 + B_\varphi^2)^{\frac{1}{2}}$. Note that the distribution of B_r contains a suggestion of a smaller peak near $B_r = -2\gamma$ as well as the more obvious peak near $B_r = +2\gamma$. During Solar Rotation Period 1799, the heliocentric range of Mariner 4 increased from $157 \cdot 10^6$ km to $169 \cdot 10^6$ km.

In Figure 9 distributions of the same quantities recorded for Solar Rotation Period 1802, 29 March through 24 April, 1965, are shown. During this period, the heliocentric range of the spacecraft increased from $197 \cdot 10^6$ to $210 \cdot 10^6$ km. Thus, the range during Period 1802 was roughly 1.25 times greater than that during 1799.

The magnitudes of the various components and the field strength are, on the average, smaller than those for Period 1799. Similarly the distributions are narrower. Since the indices of solar activity were similar during these two periods, most of the significant differences between these two sets of distributions may be the effects of radial gradients in the interplanetary field. However, the changes in the relative

preferences of the field for positive and negative values of B_r and B_φ may be the result of changes in the polarity distribution of the chromospheric fields. In this connection, it would be useful to determine whether the distribution of polarities of the solar fields or of the interplanetary field nearer the orbit of earth was changing.

The distributions also indicate that variations in the magnitudes of the various components of the field are greater than the variations in B, suggesting that the field variations are for the most part produced by changes in the orientation of a relatively constant field. However, the greatest contribution to the variations of B_r and B_φ arises from the polarity reversals of the roughly spiral field. Another property of the field, evident in both sets of distributions is the preference of B_ϑ for small positive values.

Figure 10 contains plots of similar distributions that were of measurements made with the Mariner 2 magnetometer during Solar Rotation Period 1768, 23 September through 19 October, 1962. During this period, the heliocentric range of Mariner 2 decreased from $146 \cdot 10^6$ km to $136 \cdot 10^6$ km. A comparison of the Mariner 2 results for this period with the Mariner 4 results for Period 1799, after account is taken of the effects expected due to the differences in the heliocentric ranges, suggests that somewhat greater field strengths and somewhat larger variations were produced during the earlier period. These conditions may be typical of the more active parts of the solar cycle.

DIRECTION OF THE INTERPLANETARY FIELD

Figure 11 contains plots of the distributions of

$$\alpha_B = \tan^{-1} (-B_\varphi / B_r)$$

Two of the distributions correspond to measurements that were obtained with the Mariner 4 magnetometer during the Solar Rotation Periods 1799 and 1802. The measured values of α_B may be compared with the values expected for an interplanetary field that approximates the spiral field described by Parker [1958]. According to Parker's model, at the point (r, θ, φ), the angle from the radial direction to the direction outward along the spiral field is given by

$$\alpha_p = \tan^{-1} \left[(\omega_S r \sin \theta) / V_p \right] \qquad (1)$$

where ω_S is the angular velocity of rotation of the sun, roughly $2.90 \cdot 10^{-6}$ rad/sec, and V_p is the velocity of the solar wind, assumed to be radially outward from the sun. Thus, for the spiral field, $\alpha_B = \alpha_p$ or $\alpha_p + 180^\circ$. Although detailed data on the velocity of the solar wind are not yet available, preliminary results from the plasma probe on board Mariner 4 indicate that V_p ranged from 285 to 600 km/sec with an average somewhat below 400 km/sec during the first few months of the flight [Dr. C. W. Snyder,

private communication]. Thus, a value of $\alpha_p \approx 40^\circ$ will be used here for purposes of comparison. The peaks in the distribution of α_B in Figure 11 are fairly close to the expected values of 40° and 220°. During both these periods, the component in the $r\varphi$ plane was preferentially oriented in the quadrant centered about the expected value of α_p. However, during the later period the preference for this quadrant was considerably greater.

This distribution for α_B obtained in 1962 during Solar Rotation Period 1768 with the Mariner 2 magnetometer is also shown in Figure 11. During this period, the average value of V_p was about 500 km/sec [Snyder, Neugebauer, and Rao, 1963]. The average value of α_p was approximately 50°. The peaks in the distribution of α_B are again consistent with the expected average values of 50° and $50^\circ + 180^\circ = 230^\circ$.

According to the spiral-field model, the values of B_θ should be zero. However, as mentioned previously, the distributions for B_θ extracted from both the Mariner 4 and the Mariner 2 data show that the preferred value of B_θ is typically about $+1\gamma$, indicating that the interplanetary field has a rather persistent southward component.

RADIAL GRADIENTS IN THE INTERPLANETARY FIELD

The spiral field model and the possibility that the interplanetary fields are 'frozen' into a radially flowing plasma in the solar wind suggest specific radial gradients for the quiet field, e.g., the magnitude of B_r should vary as r^{-2} while those of B_θ and B_φ should vary as r^{-1}. Similarly, the gradients produced by any irregularity frozen into the field should decrease with increasing r. Such irregularities should produce temporal variations at the position of the spacecraft as the solar wind flows past, so that variations in the radial gradients within an element of volume moving with the plasma may be detected. Similarly, azimuthal gradients in the field configuration that effectively rotates with the sun would produce temporal variations in the field recorded at the slowly moving spacecraft. In either case, for frozen-in fields, in a radially expanding plasma, one would expect the measured variations, averaged over long periods, to be smaller if they are measured in greater heliocentric ranges. For the quiet field, the magnitudes of the standard deviations would vary as r^{-2} for $B_r(t)$ and as r^{-1} for $B_\theta(t)$ and $B_\varphi(t)$, where r is the heliocentric range at which the fields are measured.

Decreases of the magnitudes and variances of the various components with increasing radial distance are suggested by the distributions shown in Figures 8 and 9. Table 1 contains a list of these quantities obtained during the other periods of solar

Table 1. Mean values and standard deviations for various components of the interplanetary field for the indicated periods of solar rotation. The heliocentric range of the spacecraft is also given for the midpoint of each period.

Solar Rotation Period No.	Starting Date (Mo./Day) GMT	Mean (gammas)		Standard Deviations (gammas)					Range
		B_P	B	B_r	B_θ	B_φ	B_P	B	(10^6km)
1798	12/12	3.5	4.5	2.8	2.3	3.2	1.9	1.8	152
1799	01/07	3.5	4.5	2.5	2.5	3.1	2.3	2.2	162
1800	02/03	3.5	4.6	2.8	3.0	2.4	2.2	2.3	176
1801	03/02	2.9	4.1	2.1	1.8	2.3	1.5	1.5	191
1802	03/29	2.6	3.5	1.7	1.5	2.0	1.4	1.6	204
1803*	04/25	2.3	3.2	1.8	1.4	1.8	1.3	1.4	215

* First 16 days of period.

rotation for which quick-look results are available. The expected decrease with increasing r appears in most of the field parameters listed. The precise radial dependences cannot be determined on the basis of quick-look data. However, the expected trends resulting from radial gradients are certainly present.

FLUCTUATIONS IN THE INTERPLANETARY FIELD

Power spectra of the variations in the interplanetary field are of interest in studies of the irregularities in the field. As mentioned previously, under the assumptions that the fields are frozen into a radially flowing solar wind, variations in the field recorded at Mariner 4, provide information concerning gradients in the field. Studies of various spectra may also permit us to determine whether local instabilities contribute significantly to the irregularities.

The quick-look data employed in obtaining the results presented here include only a few periods, of any length, over which all the measurements were available. Thus, the power spectra of the various components of the field were roughly approximated from the mean values of the variances taken over periods of various lengths.

For example, let the variance of B, over the period $4^i \cdot 12.4$ sec be denoted by $\sigma_i^2(B)$. Here i is a positive integer. Let the average of this variance for 27 days be denoted by $< \sigma_i^2(B) >$. The average power in the frequency components of B(t) with frequencies f above $f_i = 4^i \cdot 12.6)^{-1}$ cps is assumed to be approximately $< \sigma_i^2(B) >$. The average power in the range of frequencies from f_i to f_{i+1} then may be approximated by $< \sigma_{i+1}^2(b) > - < \sigma_i (B) >$. The period of 12.4 seconds is that required to obtain four consecutive measurements of the field

vector when the data rate of the Mariner 4 telemetry system was 33 1/3 bps (bits per sec), i.e., from launch until 3 January 1965. After this time the data rate and the sampling rate of the magnetometer were reduced by factors of four.

Spectra of $B_r(t)$ and $B(t)$, obtained in this manner, for Solar Rotation Periods 1799 and 1802, are shown in Figure 12. The decrease in the power in the spectra for Period 1802, relative to the corresponding spectra for Period 1799, is presumed to be due to the increase in the heliocentric range at which the latter measurements were obtained.

These relatively crude spectra also suggest that very little power is associated with the variations at frequencies above $f_2 = (1/50.4)$ cps. The measured values of the field components were converted to integral numbers on board the spacecraft for transmission by the digital telemetry system. The range of field strength that corresponds to each number was 0.7γ. Thus, the uncertainity of each measurement was 0.35γ corresponding to a field equivalent noise power about $0.12\gamma^2$. But this value is very nearly that associated with the frequencies above (1/50.4) cps.

VARIATIONS IN THE POLARITY DISTRIBUTION

A comparison of the data obtained with the magnetometers on board Mariner 2 and Mariner 4 yields evidence for a significant change in the distribution of polarities in the interplanetary magnetic field between November, 1962, and November, 1964.

For the purposes of this section the results of interest from Mariner 2 experiment were those obtained during Solar Rotation Periods 1767 through 1769. Mariner 4 was launched late in Period 1797 so that the data obtained through Period 1802 were employed in this comparison. More specifically, the Mariner 2 results were obtained between 29 August and 15 November, 1962. The results from Mariner 4 were only those obtained between 30 November, 1964, and 1 March 1965.

According to Snyder, Neugebauer, and Rao [1963], the average value of V_p, measured by the plasma probe on board Mariner 2, was about 500 km/sec. Thus, for the period of interest the average value of α_p (See Equation 1) was roughly 40°. In the following, the polarity of the interplanetary field will be reckoned positive for $-50^\circ \leq \alpha_p \leq 130^\circ$ and negative for the remaining 180° range. This criterion was applied to the Mariner 4 measurements also, because detailed measurements of V_p were not available.

For each three-hour period, the distribution of α_B was obtained. (Figure 11 contains distributions for 27-day periods)

From each such distribution, the most frequently occuring ten-degree range of α_B was determined. These values, the modes of the distributions, are plotted versus time in Figures 13 and 14. Figure 13 contains the results from Mariner 2. Figure 14 contains those from Mariner 4. No attempt has been made here to accurately determine the expected differences in the times of disturbances at the spacecraft and at the earth. However, for the ranges of V_p recorded, these differences would have been less than 1.5 days for any disturbance propagating spherically at the velocity V_p. Further, the differences for a disturbance source rotating with the sun would not have exceeded 0.5 days.

As reported previously [Davis, 1965; Davis, Smith, Coleman, and Sonett, 1964], the Mariner 2 data, plotted in Figure 13, indicate two polarity reversals during each period of solar rotation. One occurred on the fifteenth day of both Periods 1767 and 1768. (The instruments were not operating during the period from Day 305 - 311.) The time of the other reversal, relative to the solar rotation period, is not as sharply defined, since the reversal occurred on the second day of Period 1768 and on the third day of 1769. The Mariner 4 data plotted in Figure 14 show reversals occurring more frequently, although most of the reversals are not as sharply defined during the Mariner 2 flight. Further, the stability of the orientation is, in general, much less during the Mariner 4 flight.

Ness and Wilcox [1965] reported that the polarity reversed

four times during each 27-day period between December 1963, and February, 1964. The times assigned to the reversals appear from the report to be the third (+ to -), sixth (- to +), fourteenth (+ to -), and twenty-second (- to +) days of the solar rotation period. These observations were based upon measurements obtained with the magnetometer on board the earth satellite IMP-1, during periods in which the satellite was outside the magnetosphere and the region of interaction between the magnetosphere and the interplanetary medium.

In considering the lifetimes of the regions producing these effects, a comparison of the times of occurrence and signs of the reversals observed during the three flights is of interest. A polarity change from positive to negative occurred on the sixteenth day of the solar rotation period during the Mariner 2 flight, on the fourteenth day during the IMP flight and on the sixteenth day of Period 1798 during the Mariner 4 flight. However, no such change occurred during Period 1799, and, although it occurred during the seventeenth day of Period 1800, the duration of the resulting negative polarity was relatively short. Reversals on the twenty-third day (- to +) of Period 1798, on the second day (+ to -), and the seventh day (- to +) of Period 1799, lead to the speculation that a specific 27-day polarity distribution may have predominated during the period from December 1963 to February 1965.

Dodson, Hedeman, and Stewart [1965] have provided data on solar activity which indicate that the period May-November, 1964

was probably a period of minimum solar activity and that July was the quietest month in the period. The flight of Mariner 2 preceded this period by about 2 years, but the flight of IMP-1 preceded the time of this minimum by about six months and the flight of Mariner 4 followed it by about five months. Thus, a relatively stable distribution of polarities in the interplanetary field might be expected during this part of the solar cycle. However, an analysis beyond the scope of this preliminary work will be required to separate the effects of short-lived, active regions on the sun from possible effects with relatively stable sources.

Acknowledgements

The efforts of many individuals on the Mariner project team at Jet Propulsion Laboratory, contributed to this experiment. In particular, J. Lawrence and D. Norris served as Cognizant Engineers for the magnetometer at the Jet Propulsion Laboratory. The instrument was developed and fabricated at Texas Instruments, Inc., under the direction of F. Riley.

This work was supported by the National Aeronautics and Space Administration under the following research grants and contracts: NGR-05-007-065 (P.J.C.), NASw-6 (E.J.S.), NsG 426 (L.D.), and NGR-45-001-011 (D.E.J.).

BIBLIOGRAPHY

Axford, W. I., H. E. Petschek, and G. L. Siscoe, Tail of the Magnetosphere, J. Geophys. Res, 70, 1231, 1965.

Cahill, L., Preliminary Results of the Magnetic Field Measurements in the Tail of Geomagnetic Cavity, Trans. Amer. Geophys. Union, 45, 231, 1964.

Davis, L., Jr., Mariner 2 Observations Relevant to Solar Fields, Stellar and Solar Magnetic Fields (Proceedings, Symposium 22, International Astronomical Union, September 3, 1963), Edited by R. Lust, North Holland, Amsterdam, 1965.

Davis, L., Jr., E. J. Smith, P. J. Coleman, Jr., and C. P. Sonett, The Interplanetary Magnetic Field Measurements of Mariner 2, Trans. Amer. Geophys. Union, 45, 79, March, 1964.

Dessler, A. J., Length of Magnetospheric Tail, J. Geophys. Res., 69, 3913, 1 Oct. 1964.

Dodson, H. W., E. R. Hedeman, and F. L. Steward, Solar Activity during the First 14 Months of the International Years of the Quiet Sun, Science, 148, 1328, 4 June 1965.

Dungey, J. W., in Geophysics, The Earth's Environment, edited by DeWitt, Hieblot, and Lebeau, p. 503, Gordon and Breach, New York, N. Y., 1963.

Dungey, J. W., The Length of the Magnetospheric Tail, J. Geophys. Res., 70, 1753, 1 April 1965.

Frank, L. A., J. A. Van Allen, and E. Macagno, Charged Particle Observations in the Earth's Outer Magnetosphere, J. Geophys. Res., 68, 3543, 1963.

Heppner, J. P., N. F. Ness, T. L. Skillman, and C. S. Scearce, Explorer X Magnetic Field Measurements, J. Geophys. Res., 68, 1, 1963.

Keyser, A. R., J. A. Rice, and D. L. Schearer, Metastable Helium Magnetometer for Observing Small Magnetic Fluctuations, J. Geophys. Res. 66, 4163, 1961.

McLeod, M., R. E. Holzer, and E. J. Smith, Preliminary OGO-1 Search Coil Magnetometer Results, in press, 1965.

Ness, N. F., The Earth's Magnetic Tail, Document X-612-64-392, Goddard Space Flight Center, Greenbelt, Maryland, December, 1964.

Ness, N. F., C. S. Scearce, and J. B. Seek, Initial Results of the IMP-1 Magnetic Field Experiment, J. Geophys. Res., 69, 3531, 1964.

Ness, N. F., and J. M. Wilcox, Sector Structure on the Quiet Interplanetary Magnetic Field, Document X-612-65-157, Goddard Space Flight Center, Greenbelt, Maryland, April, 1965.

Parker, E. N., Dynamics of the Interplanetary Gas and Magnetic Fields, Astrophys. J., 128, 664, 1958.

Piddington, J. H., Recurrent Geomagnetic Storms, Solar M-Regions and the Solar Wind, Planetary and Space Sci., 12, 113, 1964.

Ruddock, K. A., Optically Pumped Rubidium Vapor Magnetometer for Space Experiments, Space Res., 2, 692, 1961.

Smith, E. J., A Comparison of Explorer VI and Explorer X Magnetometer Data, J. Geophys. Res., 67, 2045, May, 1962.

Smith, E. J., L. Davis, Jr., P. J. Coleman, Jr., and C. P. Sonett, Magnetic Measurements Near Venus, J. Geophys. Res., 70, 1571, 1965.

Snyder, C. W., M. Neugebauer, and U. R. Rao, The Solar Wind Velocity and Its Correlation with Cosmic-Ray Variations and with Solar and Geomagnetic Activity, J. Geophys. Res., 68, 6361, 15 Dec. 1963.

Spreiter, J. R., and W. P. Jones, On the Effect of a Weak Interplanetary Magnetic Field, J. Geophys. Res., 68, 3555, 1963.

FIGURE CAPTIONS

Figure 1. Simplified schematic diagram of the low-field, vector, helium magnetometer included on board Mariner 4.

Figure 2. The Mariner 4 magnetometer. The sensor is shown on the right. The electronics units are on the left.

Figure 3. Mariner 4 Magnetometer Data Acquired Near Earth. The magnitudes of the total field, $|B|$, and the radial component, $|B_r|$, which is directed outward from the sun, are shown. The ordinates are the logarithms of the fields in gamma and the abscissa is time (GMT). The geocentric distance is also indicated. Each datum is a ten minute average, centered on the time at which it is plotted. The dashed vertical lines labelled 1, 2, and 3 mark transitions separating the observed data into four different field regimes.

Figure 4. Mariner 4 Near-Earth Trajectory. The left-half figure is essentially a polar plot of geocentric distance and the corresponding sun-earth-Mariner angle. Thus, this view of the trajectory is not a simple projection into a fixed plane such as the ecliptic. The circled numbers identify the positions, along the trajectory, of the 3 transitions shown in Figure 1. The dashed IMP-1 contours indicate the average positions of the

shock front and magnetopause. The schematic in the right half figure relates the transitions observed by Mariner to the different regions of interaction between the solar wind and the magnetosphere.

Figure 5. Mariner data showing multiple passages of the shock front. The data were acquired over a one-hour interval when the Mariner-earth distance increased from 36 to 38 R_e. The radial field component, B_r, is parallel to the axis of Mariner which was kept continuously pointed at the sun. The spacecraft was rolling about the Z axis at a gyro-controlled rate so that sinusoidal variations appear in the two transverse field components, B_X and B_Y. Vertical lines corresponding to the instantaneous shock front position (SF) divide the data into intervals when Mariner was inside the transition region (TR) and outside the shock in the interplanetary medium (IP).

Figure 6. Colatitude, longitude, and earth-sun probe, angle versus time for the trajectory of Mariner 4. The solar equatorial coordinate system was employed.

Figure 7. Heliocentric and geocentric ranges of Mariner 4 versus time.

Figure 8. Distributions of the values of B_r, B_θ, B_φ, B_P, and B recorded during Solar Rotation Period 1799. The histogram indicates the actual numbers of occurrences in the indicated ranges. The point plotted in each range gives the number of occurrences averaged over the range in which it appears and the two adjacent ranges.

Figure 9. Distributions of the values of B_r, B_θ, B_φ, B_P, and B recorded during Solar Rotation Period 1802. See the caption for Figure 10.

Figure 10. Distributions of the values of B_r, B_θ, B_φ, B_P, and B recorded during Solar Rotation Period 1768. These results were obtained in 1962 with the magnetometer on board Mariner 2.

Figure 11. Distributions of the angle α_B, the 'spiral' angle of the interplanetary field, recorded during Solar Rotation Periods 1768, 1799, and 1802. The data for Period 1768 were obtained during the flight of Mariner 2. See the caption for Figure 10.

Figure 12. Estimates of the average power spectra of $B_r(t)$ and $B(t)$ for Solar Rotation Periods 1799 and 1802. The power levels shown correspond to the power in the indicated range.

Figure 13. Preferred values of α_B, the spiral angle, for three-hour periods. These results were obtained during the first three months of the flight of Mariner 2. Positive polarity is assigned to the field if $-50 \leq \alpha_B \leq 130$.

Figure 14. Preferred values of α_B, the spiral angle, for three-hour periods. These results were obtained during the first three months of the flight of Mariner 4.

VECTOR HELIUM MAGNETOMETER – SIMPLIFIED SCHEMATIC

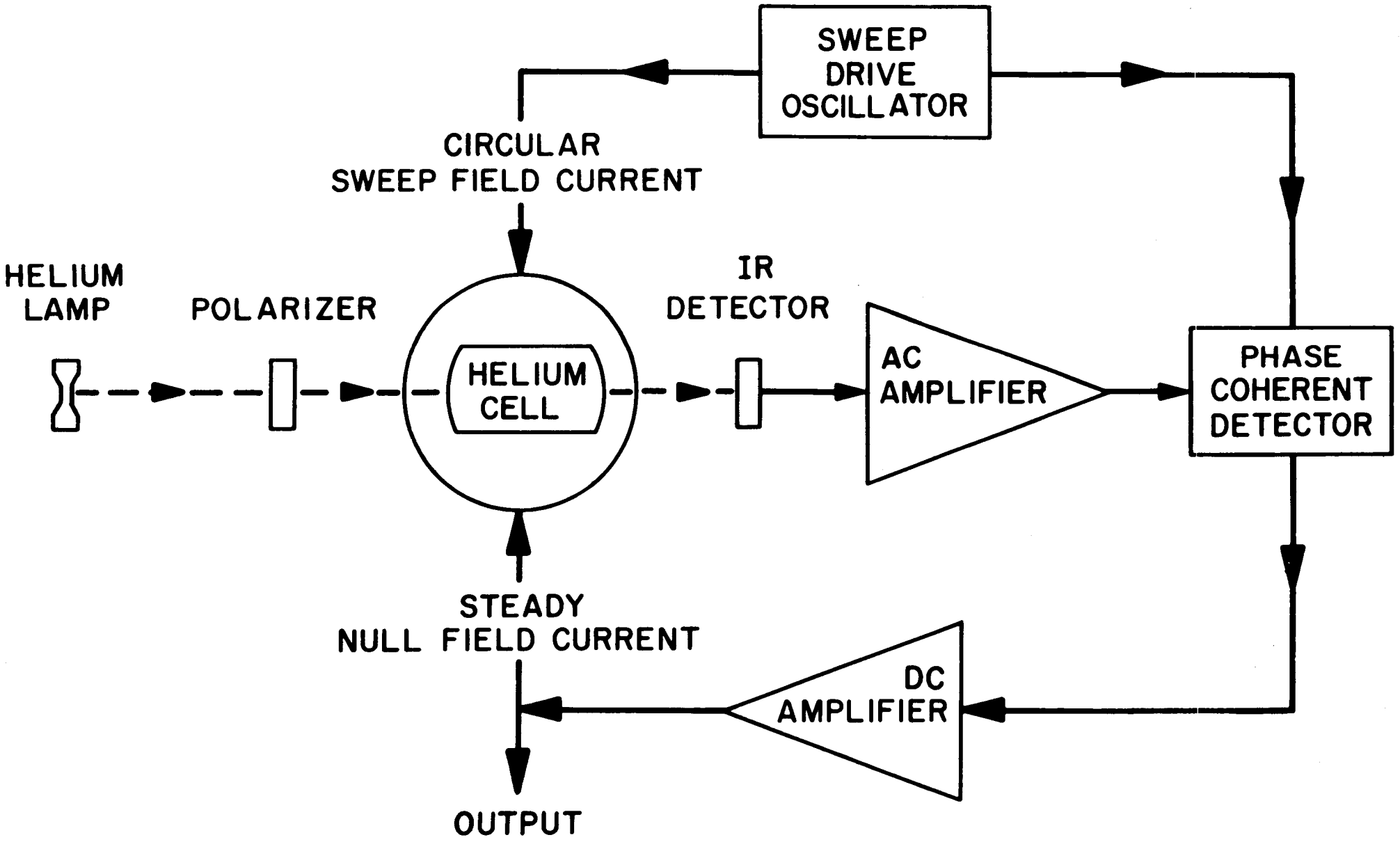

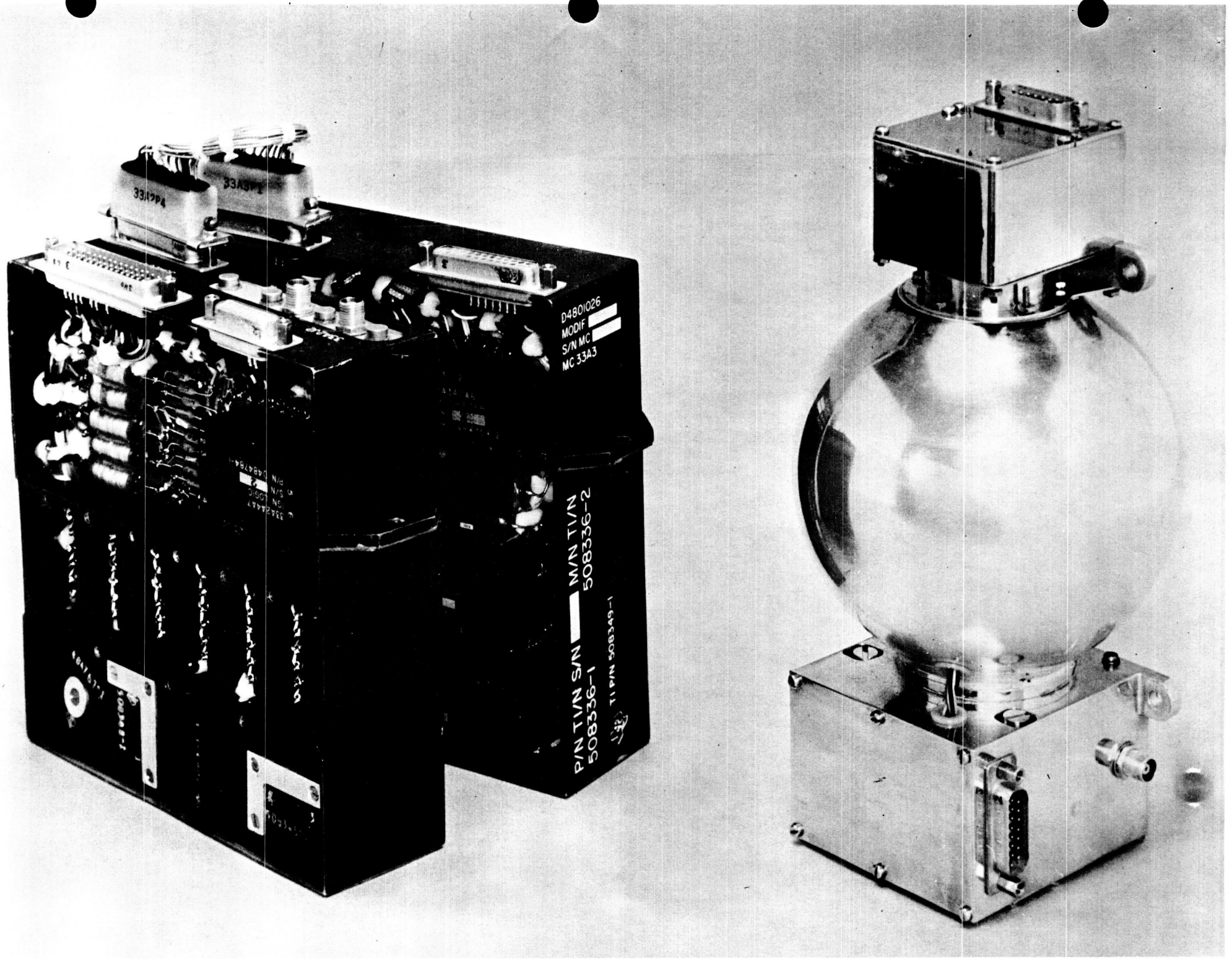
D4801026
MODIF
S/N MC
MC 33A3
P/N T/N S/N
508336-1
M/N T/N
508336-2

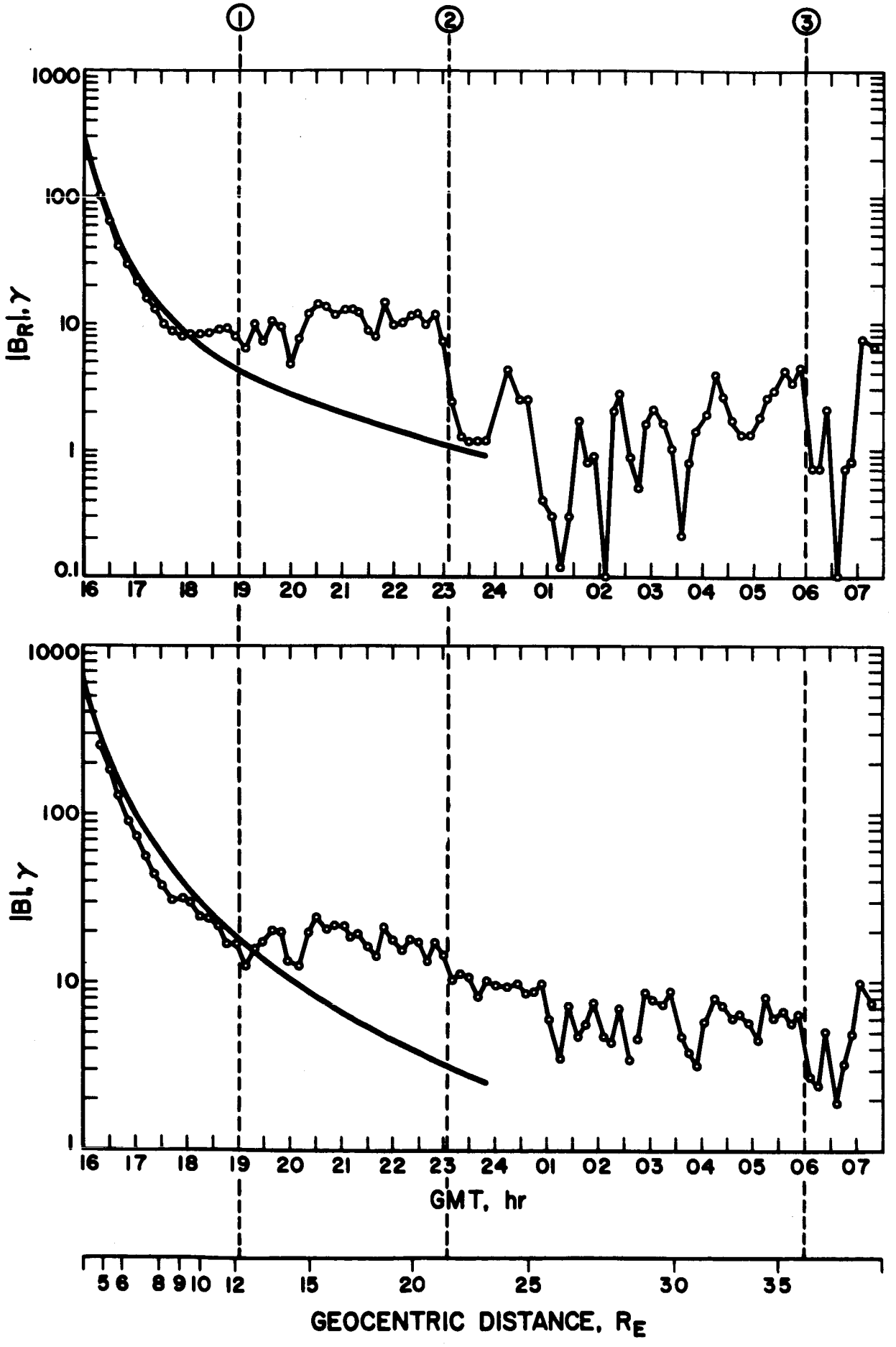

MARINER IV MAGNETOMETER DATA

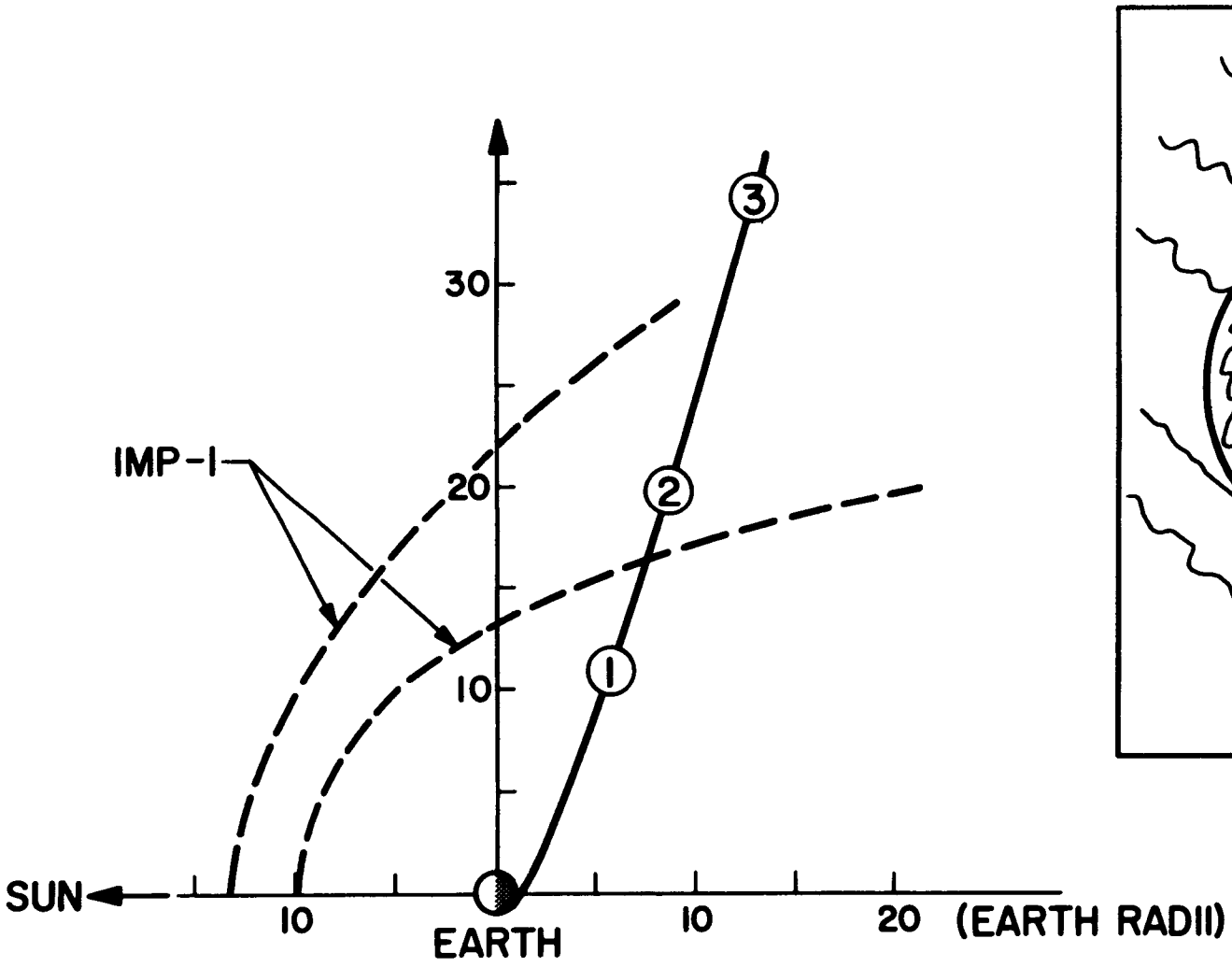

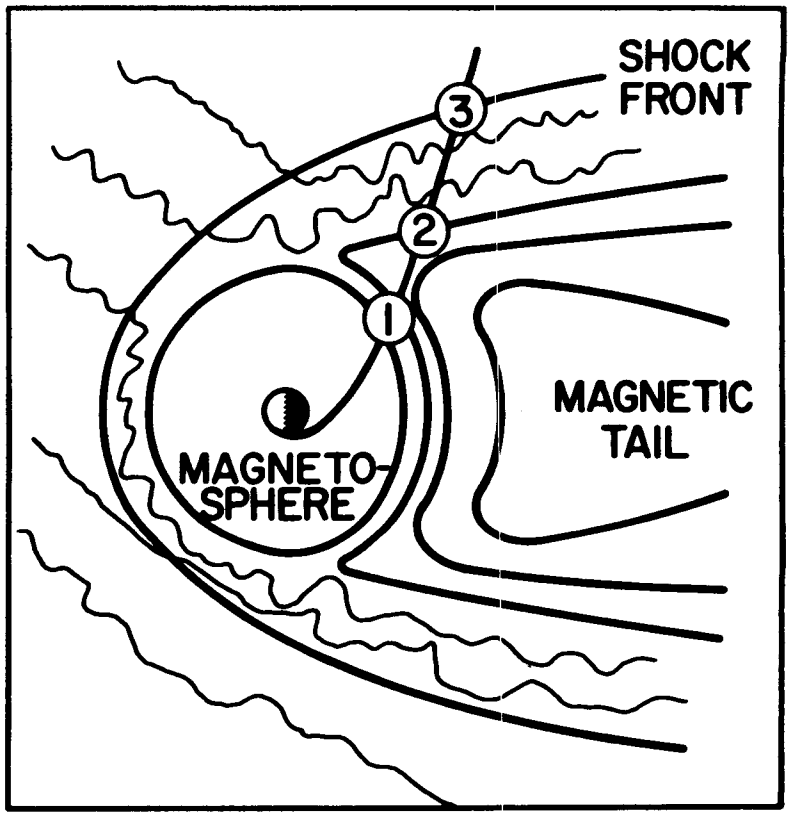

MARINER IV NEAR-EARTH TRAJECTORY

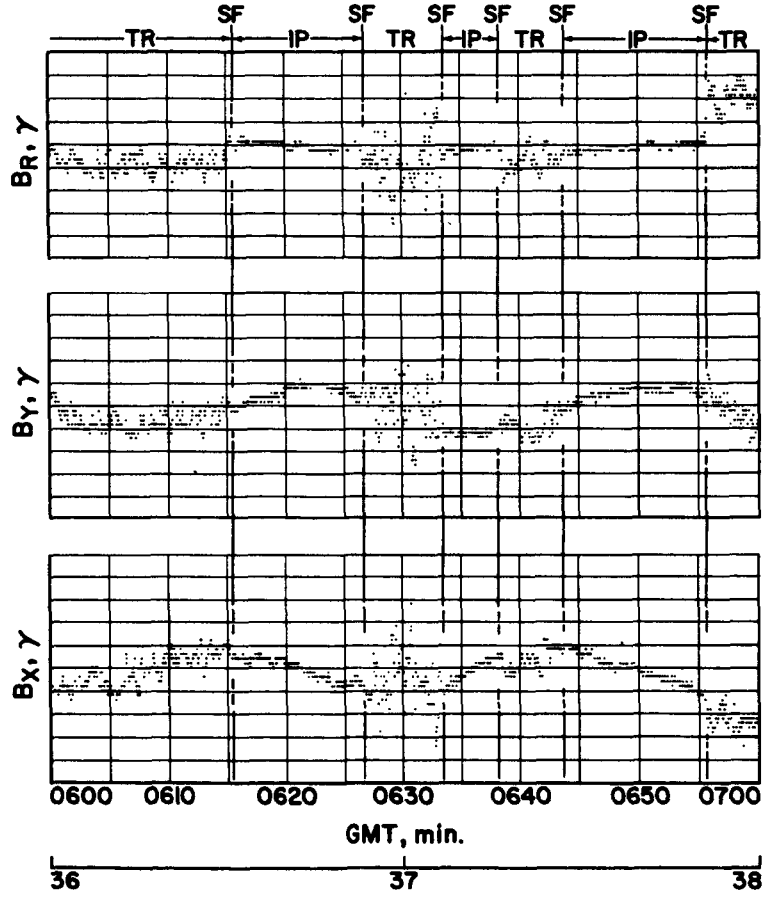

MARINER IV MAGNETOMETER DATA

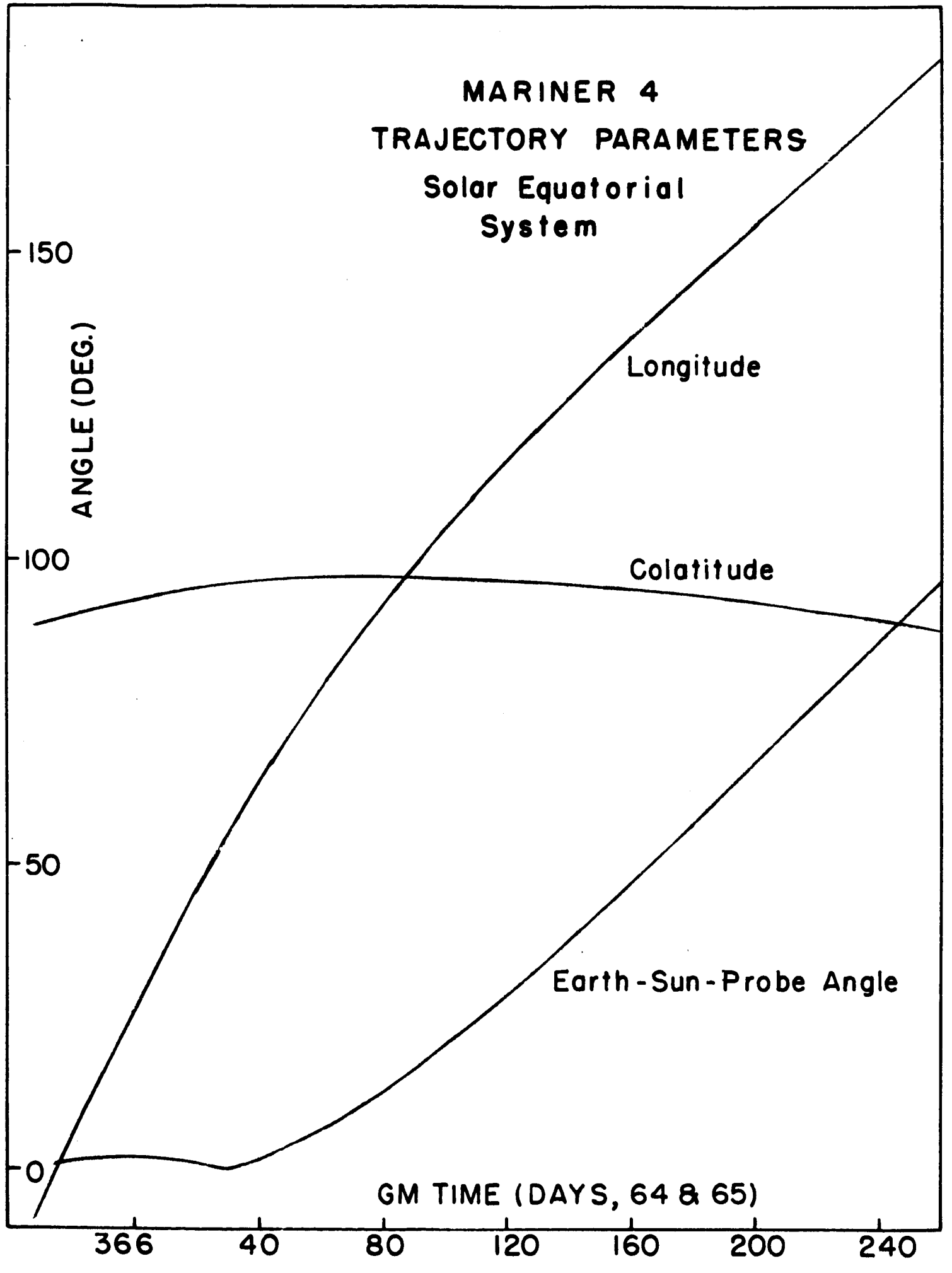
MARINER 4
TRAJECTORY PARAMETERS
Solar Equatorial
System
150
100
50
0
ANGLE (DEG.)
Longitude
Colatitude
Earth-Sun-Probe Angle
GM TIME (DAYS, 64 & 65)
366
40
80
120
160
200
240

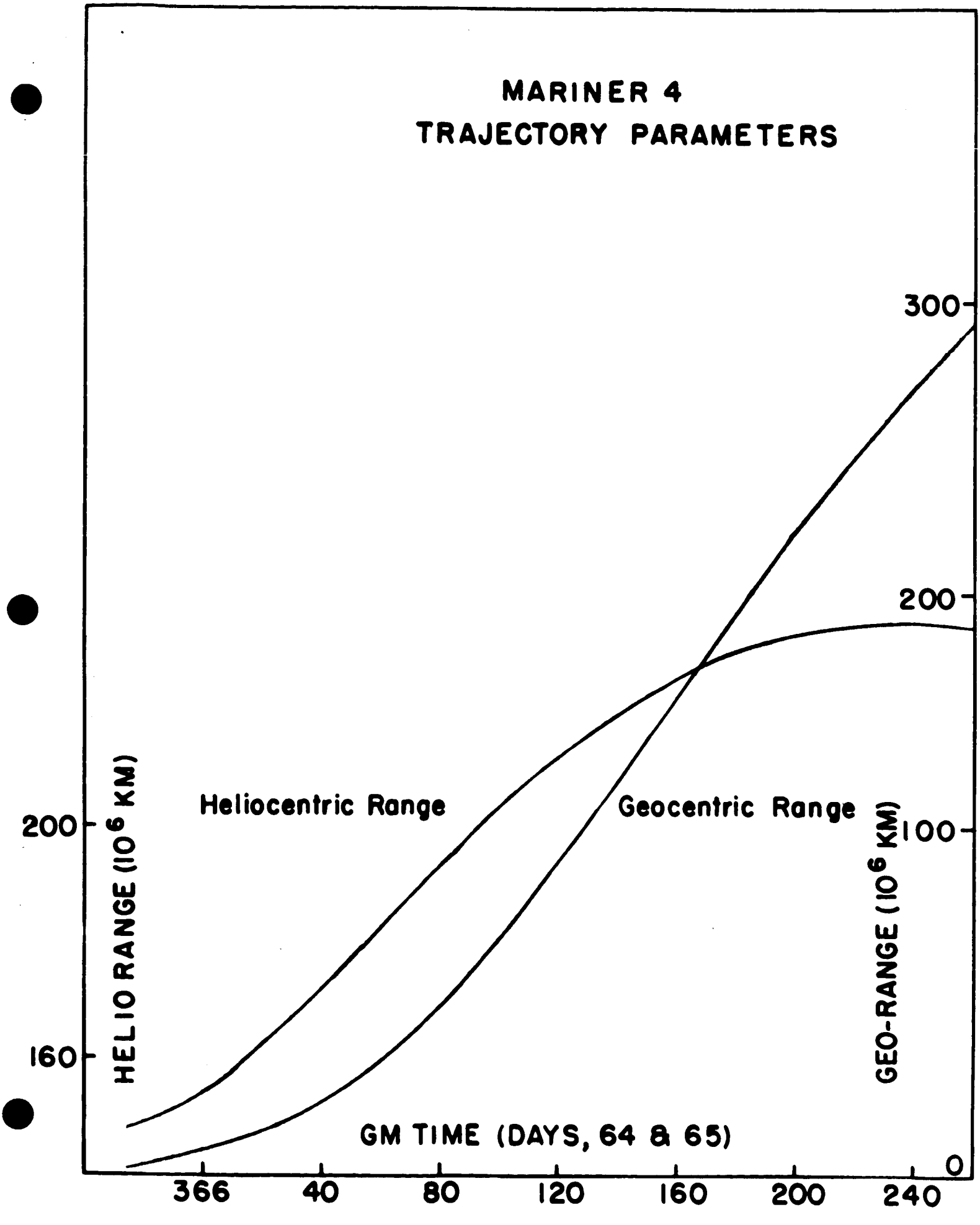
MARINER 4
TRAJECTORY PARAMETERS
300
200
100
0
200
160
HELIO RANGE (10^6 KM)
GEO-RANGE (10^6 KM)
Heliocentric Range
Geocentric Range
GM TIME (DAYS, 64 & 65)
366
40
80
120
160
200
240

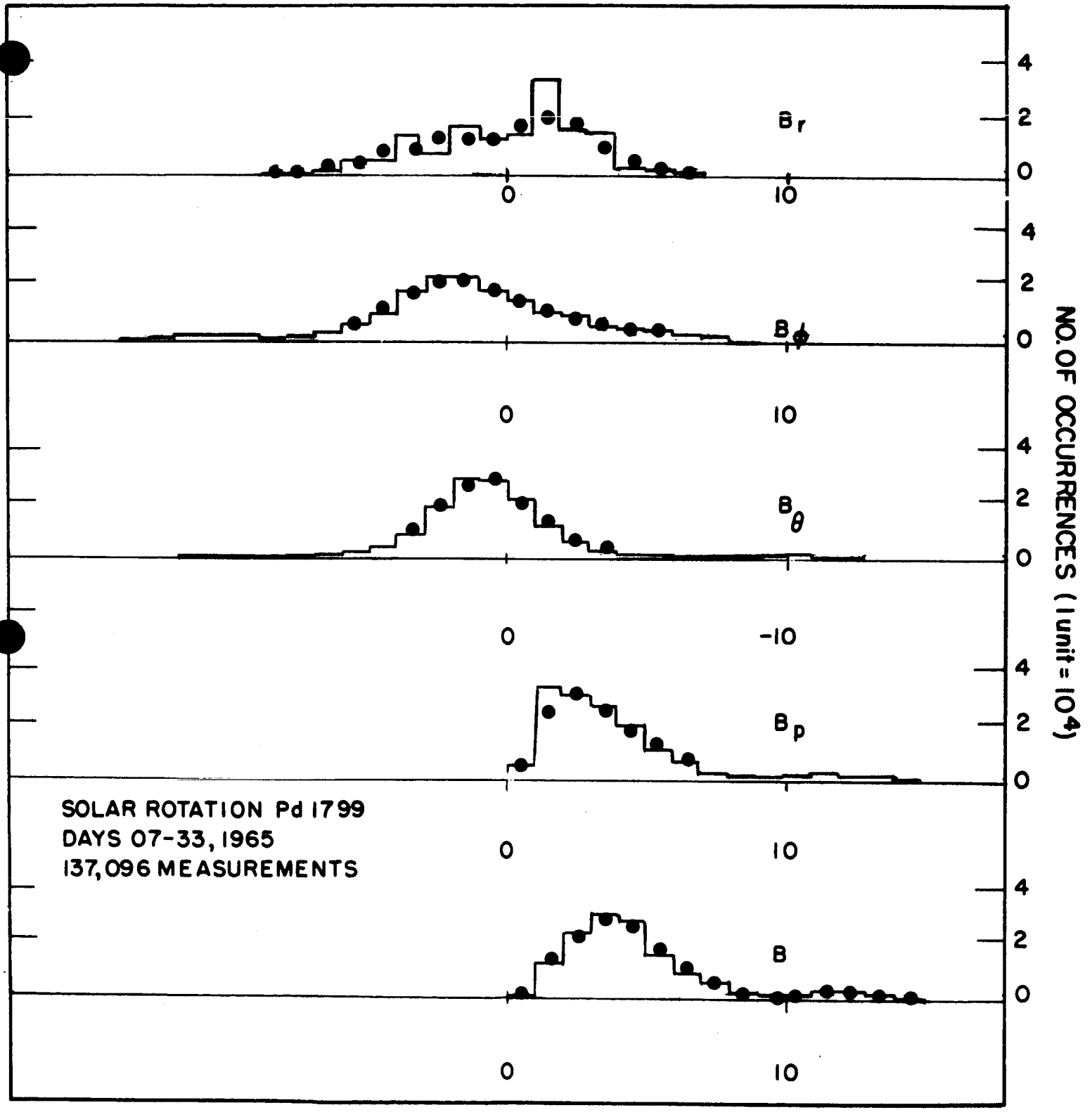

MARINER 4

DISTRIBUTIONS OF COMPONENT MAGNITUDES

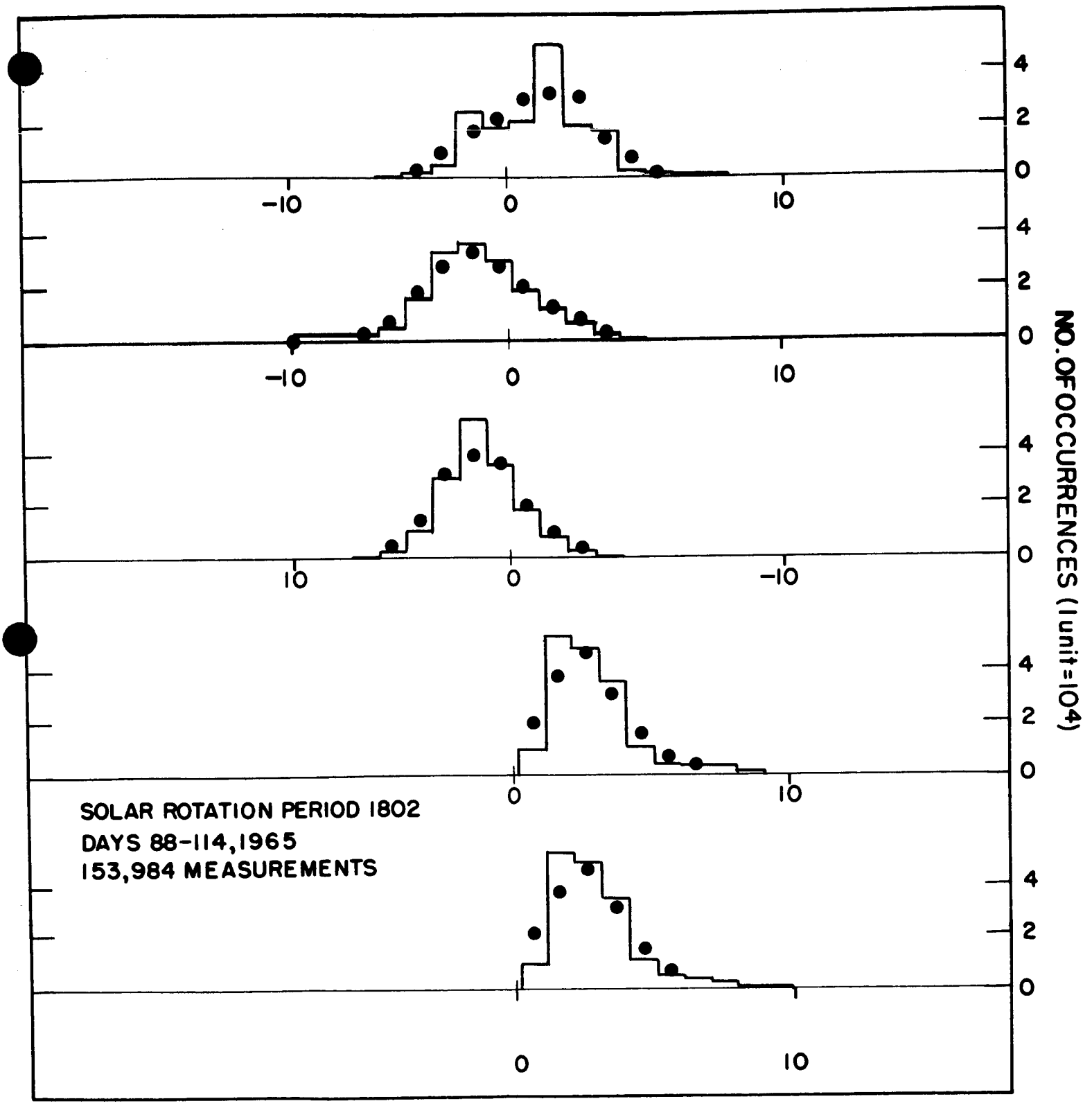

MARINER 4

DISTRIBUTIONS OF COMPONENT MAGNITUDES

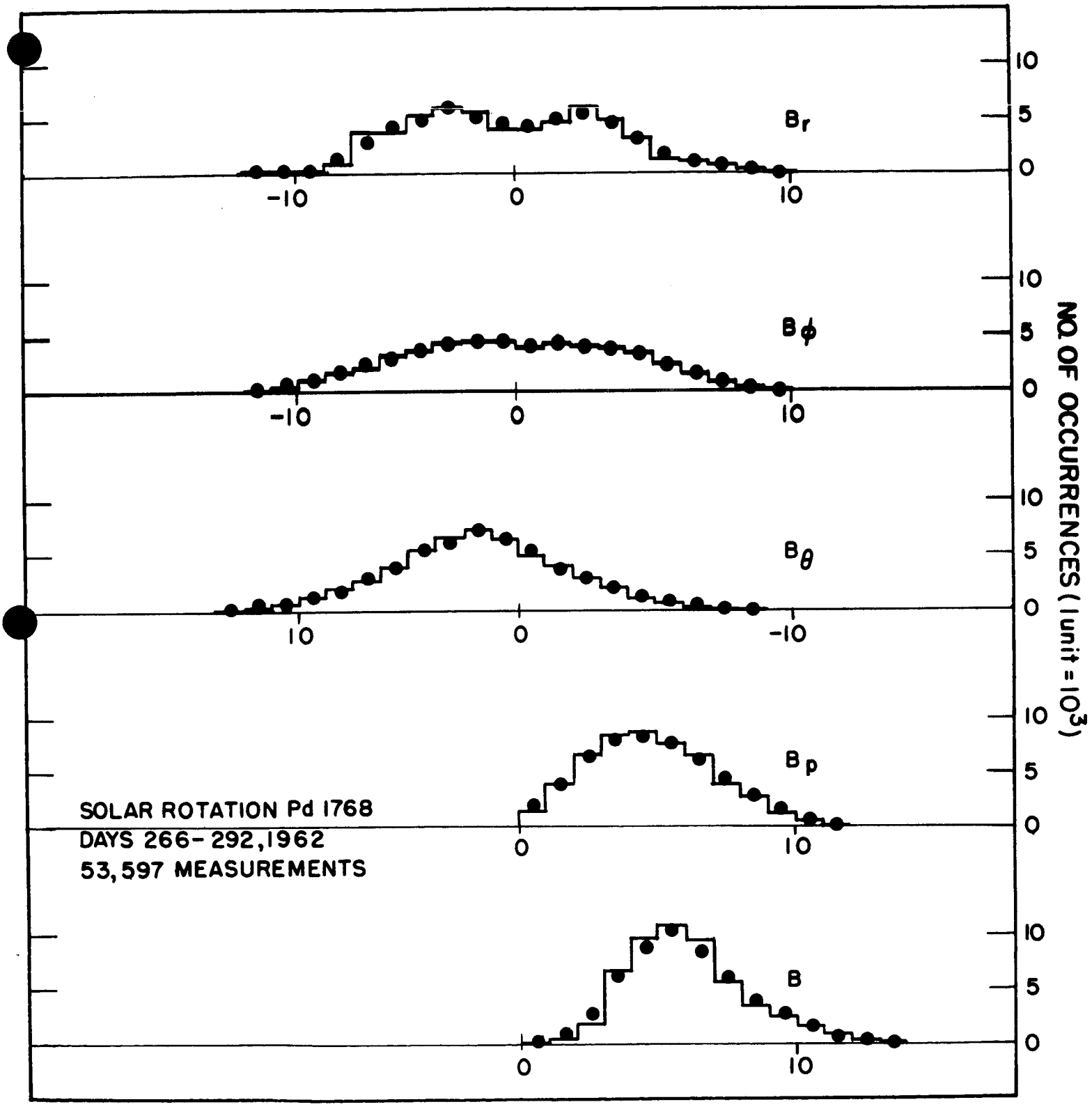

MARINER 2

DISTRIBUTIONS OF COMPONENT MAGNITUDES

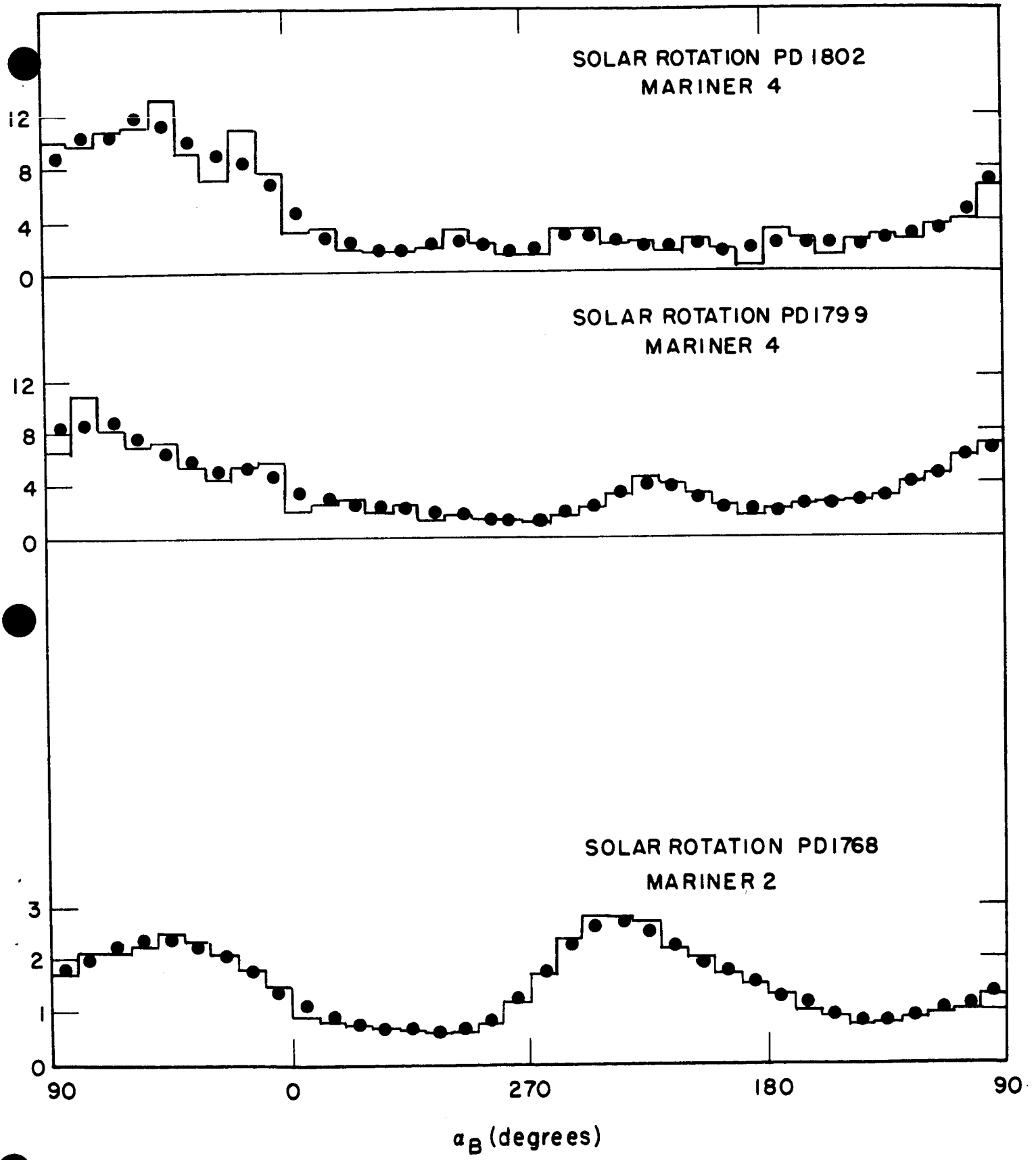

MARINER 2&4
DISTRIBUTIONS OF SPIRAL ANGLE

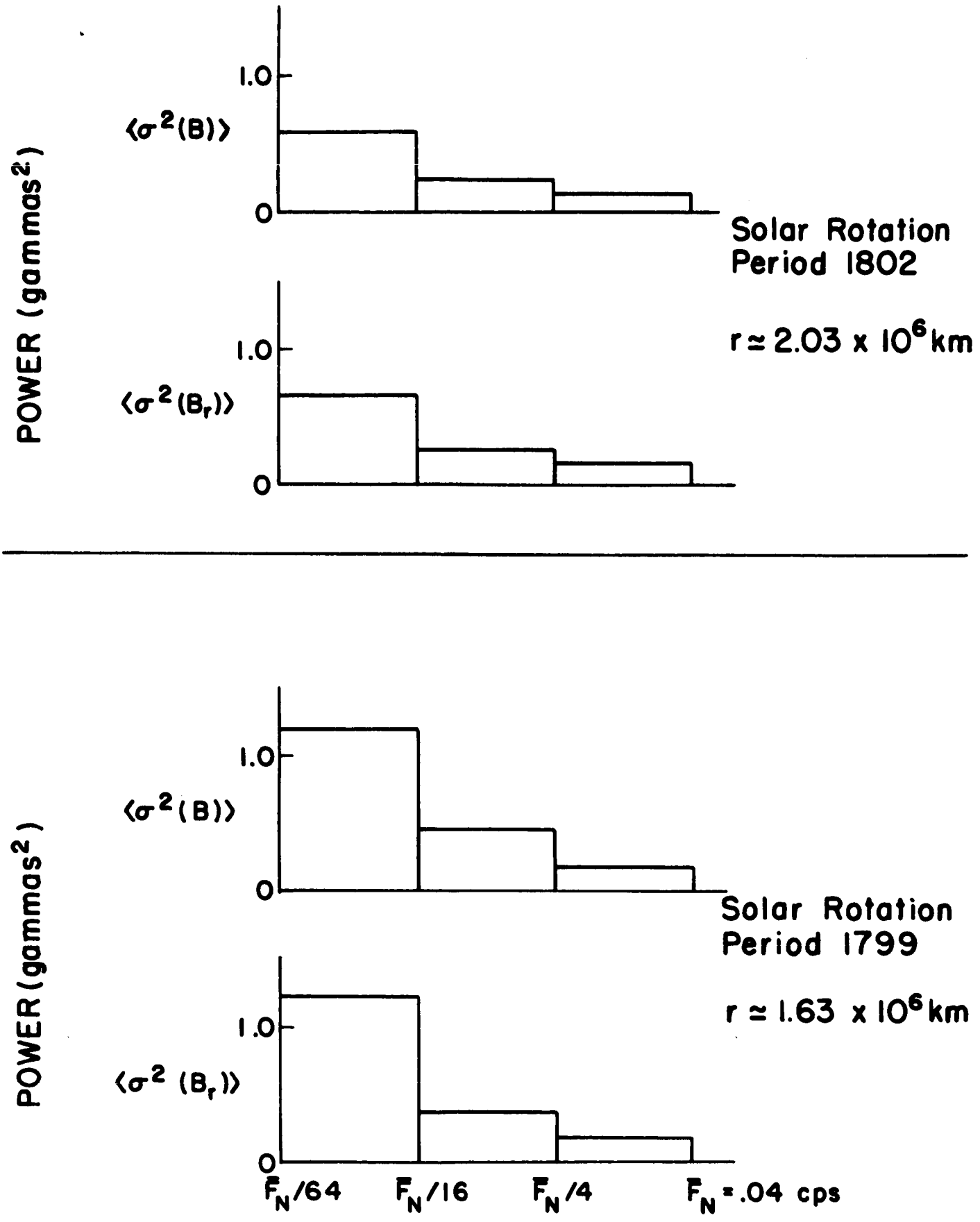

MARINER 4 APPROXIMATED POWER SPECTRA

COSPAR 12

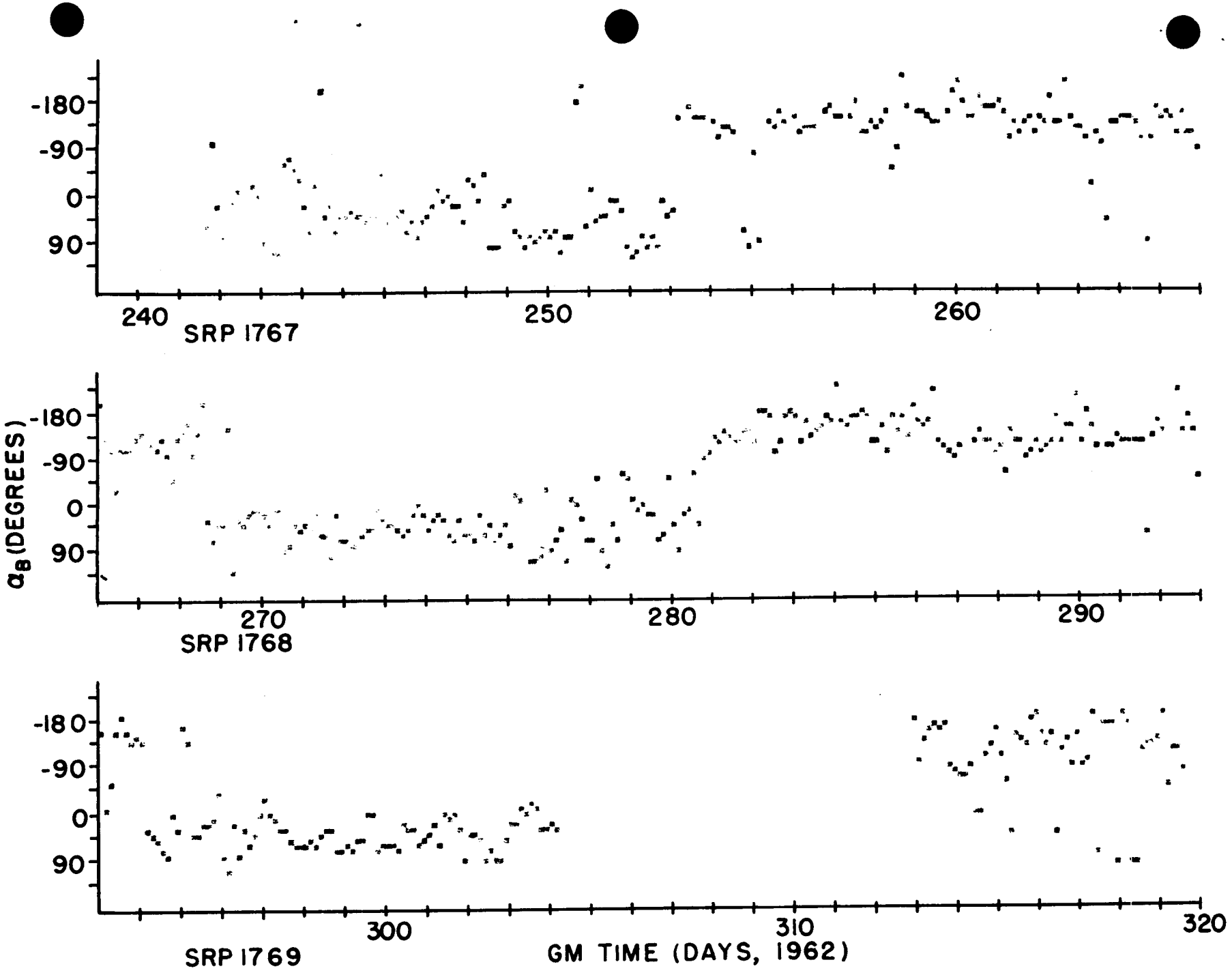

MARINER 2

SPIRAL FIELD ANGLE, PREFERRED VALUE, 3-HR PDS

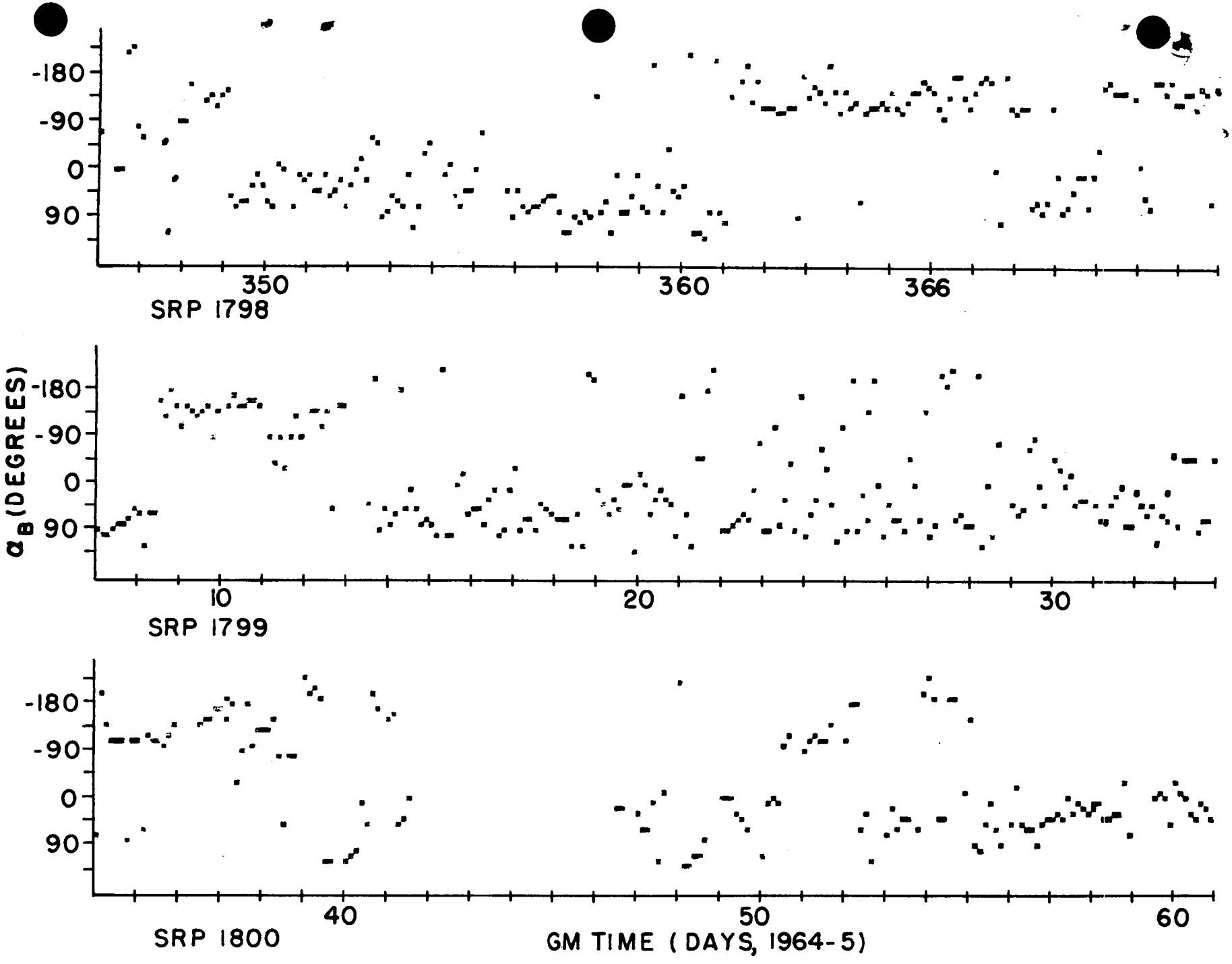

MARINER 4

SPIRAL FIELD ANGLE, PREFERRED VALUE 3-HR PDS